MULTIUSER MASSIVE MIMO DOWNLINK PRECODING USING SECOND-ORDER SPATIAL SIGMA-DELTA MODULATION

Mingjie Shao†*, Wing-Kin Ma*† *and Lee Swindlehurst*‡

†Department of Electronic Engineering, The Chinese University of Hong Kong, Hong Kong SAR of China
‡Center for Pervasive Communications and Computing, University of California Irvine, Irvine, CA 92697, USA

ABSTRACT

Massive MIMO using low-resolution digital-to-analog converters (DACs) at the base station (BS) is an attractive downlink approach for reducing hardware overhead and for reducing power consumption, but managing the large quantization noise effect is a challenge. Spatial Sigma-Delta ($\Sigma\Delta$) modulation is a recently emerged technique for tackling the aforementioned effect. Assuming a uniform linear array at the BS, it works by shaping the quantization noise as high spatial-frequency, or angle, noise. By restricting the user-serving region to be within a smaller angular region, the quantization noise incurred by the users can be effectively reduced. We previously showed that, under the one-bit DAC case, the quantization noise can be satisfactorily contained using a simple first-order $\Sigma\Delta$ modulation scheme. In this work we study the potential of spatial $\Sigma\Delta$ modulation in the two-bit DAC case and under second-order modulation. Our empirical results indicate that second-order spatial $\Sigma\Delta$ modulation provides better quantization noise suppression.

Index Terms— spatial Sigma-Delta modulation, massive MIMO, low-resolution DACs

1. INTRODUCTION

Recently, coarsely quantized massive MIMO signaling methods have generated significant interest. These methods allow us to employ low-resolution analog-to-digital convertors (ADCs)/digital-to-analog convertors (DACs) and power-efficient power amplifiers (PAs) in massive MIMO systems. As a result, the hardware cost and power consumption at the base station (BS) are tremendously reduced.

There have been a variety of studies on signal processing techniques to combat the coarse quantization for channel estimation and signal detection in uplink transmission [1–7] and more recently for downlink precoding [8–15]. Early studies directly apply the conventional linear detection/precoding techniques, e.g., zero-forcing (ZF) detector/precoder, under low-resolution ADCs/DACs. The research interest in those studies lies in characterizing the subsequent quantization noise effect; see [1,4,5] for uplink transmission and [8,10] for downlink precoding. More recently, the research focus has shifted to direct designs of the decoder and precoder to address the impact of coarse quantization. In the uplink, approximate maximum-likelihood detectors are studied in [2, 3]; in the downlink, direct one-bit precoder designs, rather than quantizing the output of an existing linear precoder, are proposed under different criteria such as mean-square-error [8, 11, 16], constructive interference [13, 17] and symbol-error-probability [12,14,15]. These approaches were empirically shown to yield improved performance, but they often involve complicated optimization.

Spatial Sigma-Delta ($\Sigma\Delta$) modulation has recently been proposed to handle the aforementioned tasks. We should mention that *temporal* $\Sigma\Delta$ modulation is a well-known quantization technique for temporal signals; see [18,19]. What we are interested is its potential in space for massive MIMO systems. Using a uniform linear array at the BS and feedback loops among adjacent antennas, the spatial $\Sigma\Delta$ modulation quantizes the signals in such a way that the quantization noise is pushed to high spatial frequencies, or angle. Thus the signals for users lying in the low spatial frequency region are less affected by the quantization noise. A number of studies have been conducted to show the efficacy of spatial $\Sigma\Delta$ modulation on signal detection [20–23], channel estimation [24] and spectral efficiency [25] in the uplink. The idea, however, is rarely exploited in the downlink [26, 27]. Our very recent study considers spatial $\Sigma\Delta$ modulation for massive MIMO downlink precoding [28]. Both the analysis and simulation results show that the first-order spatial $\Sigma\Delta$ modulation can effectively mitigate the quantization noise when the users of interest lie in a sector near the broadside of the array. Also, spatial $\Sigma\Delta$ modulation favors large numbers of antennas as in massive MIMO and closely placed antenna elements. Simple precoding designs such as ZF show competitive performance compared to the existing designs, including those that employ sophisticated optimization.

The promising results of the first-order spatial $\Sigma\Delta$ modulation motivate us to further question how its higher-order generalizations work. We answer this question by investigating second-order spatial $\Sigma\Delta$ modulation for multiuser massive MIMO downlink precoding. We show that second-order spatial $\Sigma\Delta$ modulation is more powerful in mitigating the quantization noise near the broadside. Our study also suggests that we need two-bit DACs, rather than one-bit DACs in the first-order case, to ensure safe (or no-overload) operation for the second-order spatial $\Sigma\Delta$ modulation. We extend the $\Sigma\Delta$ ZF design to the second-order case and show its connections with first-order $\Sigma\Delta$ ZF. Moreover, empirical study is conducted for overloading, e.g., employing one-bit DACs for second-order $\Sigma\Delta$ ZF. Interestingly, numerical evidence suggests that overloading may enhance the performance of $\Sigma\Delta$ ZF, which provides new insights into the practical use of $\Sigma\Delta$ ZF.

2. PROBLEM SETTINGS

Consider the downlink transmission of a multiuser massive MISO system. After propagating over a frequency-flat fading channel, the received signal at the user side can be modeled by

$$y_i = \boldsymbol{h}_i^T \boldsymbol{u} + v_i, \quad i = 1, \ldots, K, \tag{1}$$

The work of M. Shao was supported by the Hong Kong Ph.D. Fellowship Scheme. The work of L. Swindlehurst was supported by the NSF Grant ECCS-1824565.

where y_i is the received signal at user i; $\boldsymbol{h}_i \in \mathbb{C}^N$ is the downlink channel of user i; $\boldsymbol{u} \in \mathbb{C}^N$ is the transmit signal at the BS; v_i is circular complex Gaussian noise with mean 0 and power σ_v^2, i.e, $v_i \sim \mathcal{CN}(0, \sigma_v^2)$; N and K denote the number of antennas at the BS and the number of users, respectively. For simplicity, we will focus our discussion on the single-path angular channel model with a uniform linear antenna array at the BS:

$$\boldsymbol{h}_i = \alpha_i \cdot \boldsymbol{a}(\theta_i), \tag{2}$$

where $\alpha_i \in \mathbb{C}$ is the complex channel gain; θ_i is the angle of departure from the BS to user i;

$$\boldsymbol{a}(\theta) = [1, z^{-1}, \ldots, z^{-(N-1)}]^T, \quad z = e^{\mathrm{j}2\pi \frac{d \sin(\theta)}{\lambda}},$$

is the spatial signature vector; d is the inter-antenna spacing and λ is the carrier wavelength.

We consider unicast transmission, where the BS transmits separate data streams for each user. Our design seeks to achieve

$$\boldsymbol{h}_i^T \boldsymbol{u} \approx c_i s_i, \tag{3}$$

where s_i is the information symbol for user i drawn from a PSK constellation $\mathcal{S}$; $c_i > 0$ is a scaling factor. If the BS is equipped with l-bit DACs, the transmit signal $\boldsymbol{u}$ could take the form

$$\boldsymbol{u} = \beta_l \boldsymbol{x}, \quad \boldsymbol{x} = \Re\{\boldsymbol{x}\} + \mathrm{j}\Im\{\boldsymbol{x}\}, \tag{4}$$

where

$$\Re\{\boldsymbol{x}\}, \Im\{\boldsymbol{x}\} \in \mathcal{X}^N;$$

$\mathcal{X} \triangleq \{-2^l+1, -2^l+3, \ldots, 2^l-3, 2^l-1\}$; $\beta_l > 0$ is chosen to satisfy the total power constraint P assuming that the elements are uniformly distributed on $\mathcal{X}$. For example, in the one-bit DAC case,

$$\mathcal{X} = \{-1, 1\}, \quad \beta_1 = \sqrt{P/(2N)}; \tag{5}$$

and in the two-bit DAC case,

$$\mathcal{X} = \{-3, -1, 1, 3\}, \quad \beta_2 = \sqrt{P/(10N)}. \tag{6}$$

The quantization noise incurred by low-resolution DACs poses great challenges in designing $\boldsymbol{x}$ (or $\boldsymbol{u}$). In such a scenario, many of the existing works address this issue by formulating the precoding design as an optimization problem with integer variables. Herein, we resort to a different approach – spatial $\Sigma\Delta$ modulation – to alleviate the quantization noise power experienced by the targeted users.

3. REVIEW OF FIRST-ORDER $\Sigma\Delta$ MODULATION

This section will give a brief review of the basic idea of first-order $\Sigma\Delta$ modulation and its use in massive MIMO downlink precoding [28].

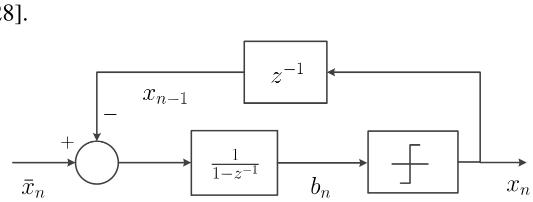

Fig. 1: System diagram of the first-order $\Sigma\Delta$ modulation.

Fig. 1 shows the system diagram of the first-order $\Sigma\Delta$ modulator. Given an input signal $\bar{\boldsymbol{x}} \in \mathbb{R}^N$, the input-output relation of the first-order $\Sigma\Delta$ modulator is expressed as

$$x_n = \bar{x}_n + q_n - q_{n-1}, \quad n = 1, \ldots, N, \tag{7}$$

where $x_n = \mathrm{sign}(b_n)$ with $b_n = b_{n-1} + (\bar{x}_n - x_{n-1})$; $q_n = x_n - b_n$ is the quantization noise. Here, the DACs applied on b_n are one-bit. The corresponding system response is given by

$$X(z) = \bar{X}(z) + (1 - z^{-1})Q(z), \tag{8}$$

where $X(z) = \sum_{n=0}^{\infty} x_n z^{-n}$ denotes the z-transform. The response $1 - z^{-1}$ corresponds to a simple high-pass filter, and thus the quantization noise is shaped towards the high frequency region. At the same time, by keeping $\bar{\boldsymbol{x}}$ in the low-frequency region, the impact of the quantization noise on $\bar{\boldsymbol{x}}$ can be mitigated.

As a key remark, to avoid unbounded quantization noise due to the feedback loop, the system should not be overloaded [18, 19]. Technically speaking, the quantization error amplitude should be limited to be within half a quantization step size, i.e., $|q_n| < 1$. This will be safely guaranteed that the input signal satisfies $|\bar{x}_n| \leq 1$ [18,28]. When the system is not overloaded, it is common to assume that the quantization noise q_n's are independent and identically distributed (i.i.d.) and uniformly distributed on $[-1, 1]$ [18].

$\Sigma\Delta$ modulation has been widely studied for quantizing temporal data. Our interest, however, lies in its use in space for massive MIMO systems under (2). In the spatial domain, spatial frequency corresponds to spectral frequency in the temporal domain. Spatial $\Sigma\Delta$ modulation pushes the quantization noise towards the high spatial frequency region. Thus users within a sector near broadside benefit most from the $\Sigma\Delta$ modulation [28]. To put this into context, with a little abuse of notation, let $\bar{\boldsymbol{x}} \in \mathbb{C}^N$ be the precoded signal to be $\Sigma\Delta$ modulated and let $\boldsymbol{x}$ be the $\Sigma\Delta$ modulator output used as the transmit signal at the BS in (4). We apply first-order $\Sigma\Delta$ modulation separately to the real and imaginary parts of $\bar{\boldsymbol{x}}$. This leads to

$$y_i = \sqrt{\frac{P}{2N}} \boldsymbol{h}_i^T \bar{\boldsymbol{x}} + w_i, \quad w_i = \sqrt{\frac{P}{2N}} \boldsymbol{h}_i^T (\boldsymbol{q} - \boldsymbol{q}^-) + v_i, \tag{9}$$

where $\boldsymbol{q} = [q_1, \ldots, q_N]^T$, $\boldsymbol{q}^- = [0, q_1, \ldots, q_{N-1}]^T$; w_i is approximated as a zero-mean Gaussian noise with power

$$\sigma_{w,i}^2 = \sigma_{q,i}^2 + \sigma_v^2, \tag{10}$$

where $\sigma_{q,i}^2 \approx \frac{4|\alpha_i|^2 P}{3} \left|\sin\left(\frac{\pi d}{\lambda} \sin(\theta_i)\right)\right|^2$ is the effective quantization noise power; see [28]. We see that $\sigma_{q,i}^2$ increases with the user angle $|\theta_i|$.

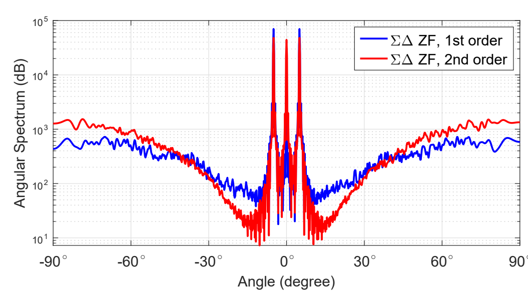

Fig. 2: Angular power spectrums of first- and second-order $\Sigma\Delta$ ZF.

To provide intuition, Fig. 2 shows the angular power spectrum $\mathbb{E}[\|\boldsymbol{a}(\psi)\boldsymbol{x}\|^2]$ over the angular range $[-90°, 90°]$ for spatial $\Sigma\Delta$ modulation. In Fig. 2, a BS with $N = 512$ antennas with spacing $d = \lambda/4$ serves $K = 3$ users at angles $-5°$, $0°$ and $5°$; the channel gains are $|\alpha_i| = 1$ for all i and phases are i.i.d. uniformly distributed on $[-\pi, \pi]$. The background noise power is zero, i.e., $\sigma_v^2 = 0$. The blue line shows the angular power spectrum of the first-order $\Sigma\Delta$ ZF precoder, which will be specified soon. The angular power spectrum consists of three spikes at the user angles and a bowl-shaped quantization noise, as the theoretical results in (9) and (10) predict.

The first-order $\Sigma\Delta$ ZF precoder is designed as [28]

$$\bar{\boldsymbol{x}} = \gamma \boldsymbol{A}^{\dagger}\boldsymbol{D}\boldsymbol{s}, \tag{11}$$

where $\boldsymbol{A} = [\boldsymbol{a}_1, \ldots, \boldsymbol{a}_K]$ and $\boldsymbol{a}_i = \boldsymbol{a}(\theta_i)$; $(\cdot)^{\dagger}$ is the Moore–Penrose inverse; $\boldsymbol{D} = \mathrm{Diag}(\sigma_{w,1}\alpha_1^*/|\alpha_1|^2, \ldots, \sigma_{w,K}\alpha_K^*/|\alpha_K|^2)$; $\boldsymbol{s} = [s_1, \ldots, s_K]^T$; $\gamma = 1/\|\boldsymbol{A}^{\dagger}\boldsymbol{D}\boldsymbol{s}\|_{IQ-\infty}$; $\|\cdot\|_{IQ-\infty}$ is defined as

$$\|\boldsymbol{x}\|_{IQ-\infty} = \max\{|\Re(x_1)|, \ldots, |\Re(x_N)|, |\Im(x_1)|, \ldots, |\Im(x_N)|\}.$$

The choice of γ ensures that the first-order $\Sigma\Delta$ modulators will not be overloaded, i.e., $|\Re\{\bar{\boldsymbol{x}}\}|, |\Im\{\bar{\boldsymbol{x}}\}| \leq \mathbf{1}$. The first-order $\Sigma\Delta$ ZF (11) also ensures that the effective SNRs of all the users are identical and given by

$$\mathsf{SNR}_{i,\mathsf{eff}} = \frac{P}{2N}\gamma^2, \quad i = 1, \ldots, K. \tag{12}$$

It can be shown that

$$\mathsf{SNR}_{i,\mathsf{eff}} \geq \mathcal{L} \triangleq \frac{PN|\alpha_k|^2\lambda_{\min}^2(\boldsymbol{R})}{2K^3\left(\frac{4|\alpha_k|^2P}{3}\left|\sin\left(\frac{\pi d}{\lambda}\sin(\theta_k)\right)\right|^2 + \sigma_v^2\right)}, \tag{13}$$

where $\boldsymbol{R} = \boldsymbol{A}\boldsymbol{A}^H/N$ and $\lambda_{\min}(\boldsymbol{R})$ is the smallest singular value of $\boldsymbol{R}$; $k = \arg\max_{i=1,\ldots,K} \sigma_{w,i}/|\alpha_i|$; see [28]. It is interesting to see that the effective SNRs increase at least linearly with the number of transmit antennas at the BS. Thus, $\Sigma\Delta$ ZF is favorable in massive MIMO scenarios.

4. SECOND-ORDER $\Sigma\Delta$ MODULATION

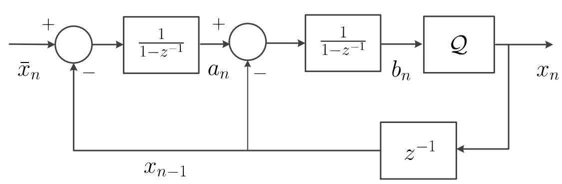

Fig. 3: System diagram of the second-order $\Sigma\Delta$ modulation.

In this section, we investigate second-order spatial $\Sigma\Delta$ modulation. The system of interest is shown in Fig. 3, and can be mathematically expressed as

$$a_n = a_{n-1} + (\bar{x}_n - x_{n-1}), \quad b_n = b_{n-1} + (a_n - x_{n-1}), \tag{14}$$

where $x_n = \mathcal{Q}(b_n)$ for some quantizer $\mathcal{Q}$, which will be specified later. At the initial stage,

$$a_{-1} = a_0 = b_{-1} = b_0 = x_{-1} = x_0 = 0.$$

Consequently, from (14) the end-to-end relation is given by

$$x_n = \bar{x}_n + q_n - 2q_{n-1} + q_{n-2}, \tag{15}$$

or, in the z-transform domain,

$$X(z) = \bar{X}(z) + (1 - z^{-1})^2 Q(z). \tag{16}$$

Here, the high-pass noise-shaping factor $(1 - z^{-1})^2$ is of higher order compared to first-order $\Sigma\Delta$ modulation (8). Thus the second-order $\Sigma\Delta$ modulation is stronger in shaping the quantization noise to high spatial frequencies. In addition, it is generally believed that the quantization noise of higher-order $\Sigma\Delta$ modulation can be more accurately characterized as i.i.d. uniform noise [18].

Similar to the first-order case, the amplitude of the input $\bar{\boldsymbol{x}}$ should be controlled such that the second-order $\Sigma\Delta$ modulator will not be overloaded. This can be guaranteed by the following:

Fact 1 *Consider the second-order $\Sigma\Delta$ modulator in* (15). *If the input signal $\bar{\boldsymbol{x}}$ satisfies $|\bar{\boldsymbol{x}}| \leq \mathbf{1}$, and the quantizer $\mathcal{Q}$ is given by*

$$\mathcal{Q}(x) = \begin{cases} -3, & \text{if } -4 \leq x < -2 \\ -1, & \text{if } -2 \leq x < 0 \\ 1, & \text{if } 0 \leq x < 2 \\ 3, & \text{if } 2 \leq x \leq 4, \end{cases} \tag{17}$$

then the second-order $\Sigma\Delta$ modulator in (15) *will not overload, i.e., $q_n \in [-1, 1]$ for all n. Moreover, if one-bit DACs are employed as the quantizer $\mathcal{Q}$, there always exists a signal $\bar{\boldsymbol{x}}$ with $|\bar{\boldsymbol{x}}| \leq \mathbf{1}$ that will overload the second-order $\Sigma\Delta$ modulator.*

The proof of Fact 1 follows the same spirit as in the first-order case [18,28]. Fact 1 suggests that 4-level (two-bit) DACs are needed to avoid overloading the second-order $\Sigma\Delta$ modulator. More generally, one can show that an M-bit DAC is sufficient to prevent overloading for an Mth-order $\Sigma\Delta$ modulator. While higher modulator orders can provide a better noise shaping, we suggest that the first- and second-order $\Sigma\Delta$ modulators can already provide reliable performance.

Applying the second-order $\Sigma\Delta$ modulation (15) in space to the downlink model (1) leads to

$$\begin{aligned} y_i &= \sqrt{\frac{P}{10N}}\boldsymbol{h}_i^T\bar{\boldsymbol{x}} + \tilde{w}_i, \\ \tilde{w}_i &= \sqrt{\frac{P}{10N}}\boldsymbol{h}_i^T(\boldsymbol{q} - 2\boldsymbol{q}^- + \boldsymbol{q}^=) + v_i, \end{aligned} \tag{18}$$

where $\boldsymbol{q}^= = [0, 0, q_1, \ldots, q_{N-2}]^T$. To avoid notational overlap, we will use the notation $\tilde{\cdot}$ to denote the variables under second-order $\Sigma\Delta$ modulation, e.g. $\tilde{w}_i$. Assuming q_n is an i.i.d. uniform sequence, the effective noise power of $\tilde{w}_i$ is given by

$$\tilde{\sigma}_{w,i}^2 = \tilde{\sigma}_{q,i}^2 + \sigma_v^2, \tag{19}$$

where $\tilde{\sigma}_{q,i}^2 \approx \frac{16|\alpha_i|^2P}{15}\left|\sin\left(\frac{\pi d}{\lambda}\sin(\theta_i)\right)\right|^4$ is the effective quantization noise power.

In the same vein as (11)-(13), we can design a ZF precoder for second-order $\Sigma\Delta$ modulation:

$$\bar{\boldsymbol{x}} = \tilde{\gamma}\boldsymbol{A}^{\dagger}\tilde{\boldsymbol{D}}\boldsymbol{s}, \tag{20}$$

where $\tilde{\boldsymbol{D}} = \mathrm{Diag}(\tilde{\sigma}_{w,1}\alpha_1^*/|\alpha_1|^2, \ldots, \tilde{\sigma}_{w,K}\alpha_K^*/|\alpha_K|^2)$ and $\tilde{\gamma} = 1/\|\boldsymbol{A}^{\dagger}\tilde{\boldsymbol{D}}\boldsymbol{s}\|_{IQ-\infty}$. Again, the effective SNR for all users is the same and given by

$$\widetilde{\mathsf{SNR}}_{i,\mathsf{eff}} = \frac{P}{10N}\tilde{\gamma}^2, \quad i = 1, \ldots, K, \tag{21}$$

which can be lower-bounded by

$$\widetilde{\mathsf{SNR}}_{i,\mathsf{eff}} \geq \tilde{\mathcal{L}} \triangleq \frac{PN|\alpha_{\tilde{k}}|^2\lambda_{\min}^2(\boldsymbol{R})}{10K^3\left(\frac{16|\alpha_{\tilde{k}}|^2P}{15}\left|\sin\left(\frac{\pi d}{\lambda}\sin(\theta_{\tilde{k}})\right)\right|^4 + \sigma_v^2\right)}, \tag{22}$$

where $\tilde{k} = \arg\max_{i=1,\ldots,K} \tilde{\sigma}_{w,i}/|\alpha_i|$. As in the first-order case, the effective SNR increases linearly with the number of antennas N at the BS.

Remark 1 An interesting question to consider is when does the second-order $\Sigma\Delta$ ZF outperform the first-order approach. Implications can be obtained by comparing the effective SNR lower bounds $\mathcal{L}$ and $\tilde{\mathcal{L}}$ in (13) and (22). By assuming $|\alpha_1| = \ldots = |\alpha_K| = \alpha$, it can be verified that $\mathcal{L} \leq \tilde{\mathcal{L}}$ when the largest angle θ_j satisfies

$$\frac{\lambda}{\pi d}\arcsin\left(\frac{1}{2\sqrt{2}}\sqrt{1-p}\right) \leq |\sin(\theta_j)| \leq \frac{\lambda}{\pi d}\arcsin\left(\frac{1}{2\sqrt{2}}\sqrt{1+p}\right), \tag{23}$$

where $p = \sqrt{1 - \frac{48\sigma_v^2}{|\alpha|^2 P}}$ given $\sigma_v^2 \leq |\alpha|^2 P/48$; $j = \arg\max_{i=1,\ldots,K} |\theta_i|$. Eqn. (23) implies that the second-order $\Sigma\Delta$ ZF will outperform the first-order $\Sigma\Delta$ ZF when 1) the background noise power σ_v^2 is sufficiently low (or when the SNR is high); and 2) when the the user angles are restricted to an interval near broadside. In the limiting case $\sigma_v^2 \to 0$, $p \to 1$, Eqn. (23) reduces to

$$\sin(\theta_j) \in \left[-\frac{\lambda}{6d}, \frac{\lambda}{6d}\right].$$

For the example in Fig. 2 where $d = \lambda/4$, the second-order $\Sigma\Delta$ would be preferred when the user angles are restricted to $[-41.8^\circ, 41.8^\circ]$.

Remark 2 Fact 1 specifies the theoretical no-overload condition of second-order $\Sigma\Delta$ modulation. However, the result may be conservative. In practice, a mild amount of overloading may not lead to quantization noise growth. It is interesting to explore the impact of overloading on second-order $\Sigma\Delta$ modulation. What will happen if we replace the two-bit DACs with one-bit DACs? What if we purposely violate the non-overload condition by feeding the modulator signals with amplitudes larger than that suggested by Fact 1? These questions will be studied by simulations in the next section.

5. SIMULATION RESULTS

This section compares the performance of the second-order $\Sigma\Delta$ ZF, the first-order $\Sigma\Delta$ ZF and the direct quantized ZF. The direct quantized ZF corresponds to using a one-bit DAC to quantize

$$\bar{\boldsymbol{x}} = \frac{\boldsymbol{H}^\dagger \boldsymbol{s}}{\|\boldsymbol{H}^\dagger \boldsymbol{s}\|_{IQ-\infty}}.$$

We consider the bit error rate (BER) performance, and the simulation settings are as follow. The number of transmit antennas at the BS and the number of single antenna users are $N = 512$ and $K = 32$, respectively. The user channel angles θ_i's are randomly picked from the range $[-30^\circ, 30^\circ]$ with inter-angle difference no smaller than 1°; the complex channel gains α_i's have phases uniformly drawn from $[-\pi, \pi]$, and amplitudes generated by $|\alpha_i| = r_0/r_i$. Here, r_i is the distance from the BS to the ith user and r_0 is the reference distance. We set $r_0 = 30$ and r_i uniformly drawn from $[20, 100]$. The results are averaged over $1,000$ channel realizations with 100 time slots per channel use. We also test two heuristics: 1) the second-order $\Sigma\Delta$ ZF using one-bit DACs, referred to as "1-bit" in the legend; 2) the overloaded second-order $\Sigma\Delta$ ZF using two-bit DACs with input signal $\bar{\boldsymbol{x}}$ in (20) amplified by a factor of $\sqrt{5}$, referred to as "OL" in the legend. The later is to make the effective signal strength at the user side in (18) comparable to that in the first-order case (9).

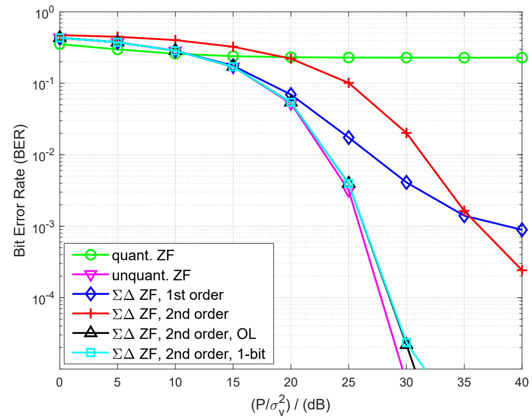

Fig. 4: The BER versus P/σ_v^2; 16-ary PSK.

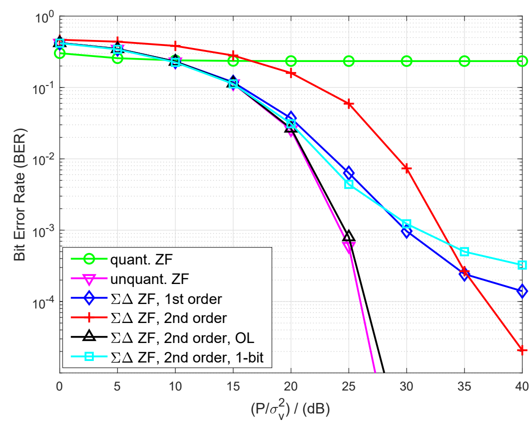

Fig. 5: The BER versus P/σ_v^2; 16-ary QAM.

Figs. 4 and 5 show the BER performance for 16-ary PSK and 16-ary QAM signaling, respectively. The second-order $\Sigma\Delta$ ZF design for QAM follows the method in [28, Section 5.3]. It is seen that both the first- and second-order $\Sigma\Delta$ ZF precoders outperform the naively quantized ZF approach. While the second-order $\Sigma\Delta$ ZF performs worse than the first-order $\Sigma\Delta$ ZF at lower SNRs, it outperforms the first-order $\Sigma\Delta$ ZF at higher SNRs. This numerical result is in agreement with our prediction in Remark 1. Interestingly, the overloaded second-order $\Sigma\Delta$ ZF "OL" achieves consistently good BER performance for both 16-ary PSK and 16-ary QAM at all tested SNRs. The second-order $\Sigma\Delta$ ZF using one-bit DACs exhibits different behavior. Its performance is comparable to that of the overloaded second-order $\Sigma\Delta$ ZF "OL" in the 16-ary PSK case, but not so impressive for the 16-ary QAM case.

6. CONCLUSION

In this paper we extended our study of spatial $\Sigma\Delta$ modulation for massive MIMO precoding to the second-order case. Second-order $\Sigma\Delta$ modulation is effective in yielding better noise shaping at lower spatial frequencies, although it also requires two-bit DACs to implement in order to avoid overloading. Insights were also provided for the comparison between first- and second-order $\Sigma\Delta$ ZF precoders. The overloaded $\Sigma\Delta$ ZF was numerically demonstrated to achieve surprisingly good BER performance in some cases.

7. REFERENCES

[1] C. Risi, D. Persson, and E. G. Larsson, “Massive MIMO with 1-bit ADC,” *arXiv preprint arXiv:1404.7736*, 2014.

[2] J. Choi, J. Mo, and R. W. Heath, “Near maximum-likelihood detector and channel estimator for uplink multiuser massive MIMO systems with one-bit ADCs,” *IEEE Trans. Commun.*, vol. 64, no. 5, pp. 2005–2018, May 2016.

[3] C. Studer and G. Durisi, “Quantized massive MU-MIMO-OFDM uplink,” *IEEE Trans. Commun.*, vol. 64, no. 6, pp. 2387–2399, 2016.

[4] Y. Li, C. Tao, G. Seco-Granados, A. Mezghani, A. L. Swindlehurst, and L. Liu, “Channel estimation and performance analysis of one-bit massive MIMO systems,” *IEEE Trans. Signal Process.*, vol. 65, no. 15, pp. 4075–4089, Aug 2017.

[5] C. Mollén, J. Choi, E. G. Larsson, and R. W. Heath, “Uplink performance of wideband massive MIMO with one-bit ADCs,” *IEEE Trans. Wireless Commun.*, vol. 16, no. 1, pp. 87–100, Jan 2017.

[6] S. Jacobsson, G. Durisi, M. Coldrey, U. Gustavsson, and C. Studer, “Throughput analysis of massive MIMO uplink with low-resolution ADCs,” *IEEE Trans. Wireless Commun.*, vol. 16, no. 6, pp. 4038–4051, June 2017.

[7] L. Fan, S. Jin, C. Wen, and H. Zhang, “Uplink achievable rate for massive MIMO systems with low-resolution ADC,” *IEEE Commun. Lett.*, vol. 19, no. 12, pp. 2186–2189, Dec 2015.

[8] S. Jacobsson, G. Durisi, M. Coldrey, T. Goldstein, and C. Studer, “Quantized precoding for massive MU-MIMO,” *IEEE Trans. Commun.*, vol. 65, no. 11, pp. 4670–4684, Nov 2017.

[9] A. Swindlehurst, A. Saxena, A. Mezghani, and I. Fijalkow, “Minimum probability-of-error perturbation precoding for the one-bit massive MIMO downlink,” in *Proc. IEEE Int. Conf. Acous., Speech, Signal Process. (ICASSP)*, Mar. 2017, pp. 6483–6487.

[10] A. K. Saxena, I. Fijalkow, and A. Swindlehurst, “Analysis of one-bit quantized precoding for the multiuser massive MIMO downlink,” *IEEE Trans. Signal Process.*, vol. 65, no. 17, pp. 4624–4634, Sept 2017.

[11] O. Castaneda, S. Jacobsson, G. Durisi, M. Coldrey, T. Goldstein, and C. Studer, “1-bit massive MU-MIMO precoding in VLSI,” *IEEE J. Emerg. Sel. Topics Circuits Syst.*, vol. 7, no. 4, pp. 508–522, Dec 2017.

[12] F. Sohrabi, Y.-F. Liu, and W. Yu, “One-bit precoding and constellation range design for massive MIMO with QAM signaling,” *IEEE J. Sel. Topics Signal Process.*, vol. 12, no. 3, pp. 557–570, 2018.

[13] H. Jedda, A. Mezghani, A. L. Swindlehurst, and J. A. Nossek, “Quantized constant envelope precoding with PSK and QAM signaling,” *IEEE Trans. Wireless Commun.*, vol. 17, no. 12, pp. 8022–8034, Dec 2018.

[14] M. Shao, Q. Li, W.-K. Ma, and A. M.-C. So, “A framework for one-bit and constant-envelope precoding over multiuser massive MISO channels,” *IEEE Trans. Signal Process.*, vol. 67, no. 20, pp. 5309–5324, 2019.

[15] M. Shao, Q. Li, Y. Liu, and W.-K. Ma, “Multiuser one-bit massive MIMO precoding under MPSK signaling,” in *Proc. IEEE Global Conf. Signal and Inf. Process. (GlobalSIP)*, Nov. 2018, pp. 833–837.

[16] S. Jacobsson, G. Durisi, M. Coldrey, T. Goldstein, and C. Studer, “Nonlinear 1-bit precoding for massive MU-MIMO with higher-order modulation,” in *Proc. Asilomar Conf. Signals, Syst. Comp.*, Nov 2016, pp. 763–767.

[17] A. Li, C. Masouros, F. Liu, and A. L. Swindlehurst, “Massive MIMO 1-bit DAC transmission: A low-complexity symbol scaling approach,” *IEEE Trans. Wireless Commun.*, vol. 17, no. 11, pp. 7559–7575, 2018.

[18] R. M. Gray, “Quantization noise spectra,” *IEEE Trans. Inf. Theory*, vol. 36, no. 6, pp. 1220–1244, 1990.

[19] P. M. Aziz, H. V. Sorensen, and J. Van Der Spiegel, “An overview of sigma-delta converters: How a 1-bit ADC achieves more than 16-bit resolution,” *IEEE Signal Process. Mag.*, vol. 13, no. 1, pp. 61–84, 1996.

[20] R. M. Corey and A. C. Singer, “Spatial sigma-delta signal acquisition for wideband beamforming arrays,” in *Proc. Int. ITG Workshop Smart Antennas (WSA)*, March 2016.

[21] D. Barac and E. Lindqvist, “Spatial sigma-delta modulation in a massive MIMO cellular system,” Master’s thesis, Department of Computer Science and Engineering, Chalmers University of Technology, 2016.

[22] A. Nikoofard, J. Liang, M. Twieg, S. Handagala, A. Madanayake, L. Belostotski, and S. Mandal, “Low-complexity N-port ADCs using 2-D sigma-delta noise-shaping for N-element array receivers,” in *Proc. Int. Midwest Symposium Circuits Syst. (MWSCAS)*, 2017, pp. 301–304.

[23] A. Madanayake, N. Akram, S. Mandal, J. Liang, and L. Belostotski, “Improving ADC figure-of-merit in wideband antenna array receivers using multidimensional space-time delta-sigma multiport circuits,” in *Proc. Int. Workshop Multidimensional (nD) Syst. (nDS)*, Sept 2017.

[24] S. Rao, A. L. Swindlehurst, and H. Pirzadeh, “Massive MIMO channel estimation with 1-bit spatial sigma-delta ADCs,” in *Proc. IEEE Int. Conf. Acous., Speech, Signal Process. (ICASSP)*. IEEE, 2019, pp. 4484–4488.

[25] H. Pirzadeh, G. Seco-Granados, S. Rao, and A. L. Swindlehurst, “Spectral efficiency of one-bit sigma-delta massive MIMO,” *arXiv preprint arXiv:1910.05491*, 2019.

[26] D. P. Scholnik, J. O. Coleman, D. Bowling, and M. Neel, “Spatio-temporal delta-sigma modulation for shared wideband transmit arrays,” in *Proc. IEEE Radar Conf.*, 2004, pp. 85–90.

[27] J. D. Krieger, C. P. Yeang, and G. W. Wornell, “Dense delta-sigma phased arrays,” *IEEE Trans. Antennas Propag.*, vol. 61, no. 4, pp. 1825–1837, April 2013.

[28] M. Shao, W.-K. Ma, Q. Li, and A. L. Swindlehurst, “One-bit sigma-delta MIMO precoding,” *IEEE J. Sel. Topics Signal Process.*, vol. 13, no. 5, pp. 1046–1061, Sep. 2019.